Soft and hard shells in metallic nanocrystals

D. Y. Sun,[1,2] X. G. Gong,[1,2] and Xiao-Qian Wang[2]
[1]*Institute of Solid State Physics, Academia Sinica, 230031-Hefei, Peoples Republic of China*
[2]*Department of Physics & Center for Theoretical Studies of Physical Systems, Clark Atlanta University, Atlanta, Georgia 30314*
(Received 24 May 2000; published 1 May 2001)

The inhomogeneous elastic properties of metallic nanocrystals are studied using semiempirical potentials for Au, Pb, Ag, and Cu. The enhanced low- and high-frequency modes are found to be spatially localized in two shells, a soft surface shell and a hard transition shell. Our analysis shows that the linear frequency dependence of the vibrational density of states is attributed to the two-dimensional nature of the surface shell that is independent of the system size, while the high-frequency tail mainly comes from the transition shell.

DOI: 10.1103/PhysRevB.63.193412 PACS number(s): 61.82.Rx, 68.35.Ja

Unusual physical and chemical properties of nanocrystals are associated with the finite-size effect, quantum-size effect, and finite surface-to-volume ratio. As a detailed understanding of the vibrational properties is the key to explain unusual thermal properties (such as the enhanced specific heat and low Debye temperature) for nanocrystals, studies on the vibrational properties of nanocrystals have spurred great scientific interest. Recent experimental and theoretical work has shown remarkable differences between the vibrational density of states (DOS) of nanocrystal and bulk materials.[1–12] The distinct features of nanocrystals entail to the enhancement of the low- and high-energy modes; the DOS of surface atoms of metallic nanocrystals at low-frequency region changes its dependency on frequency from quadratic to linear.[2,3]

For the enhanced low-frequency modes, Fultz and co-workers[6] suggested that the enhancement of the vibrational DOS at low frequency involves movements of the nanocrystals with respect to one another; while others[1,8–10] suggested that the low-frequency modes could involve vibrations of atoms within the grain boundaries or interfaces. More recent work extracts these low-frequency modes from the surface of nanocrystals.[2,3,11] For the enhancement of high-frequency modes, both short vibrational lifetime in nanocrystals due to the finite size[5–7,10,11] and the shortening of the nearest-neighbor distances[1,2] are considered. However, it remains open questions as to what is the real origin of the linear frequency dependence of surface DOS, and if the high-frequency modes are only due to the shortening of the nearest-neighbor distances.

In this paper, we report results on the local elastic and vibrational properties of metallic nanocrystals. We find that the elastic properties of metallic nanocrystals are highly inhomogeneous. The enhanced high- and low-frequency modes are localized in two thin shells. The spatially-localized nature of the modes is useful in interpreting the linear frequency dependence of the vibrational density of states (DOS) at low frequencies, predicting the size dependence of the enhanced high- and low-energy vibrational modes.

We have carried out calculations on Au, Pb, Ag, and Cu nanocrystals with different sizes. The interatomic interactions are described by well-tested many-body potentials, namely, glue potentials for Au (Ref. 13) and Pb (Ref. 14), Sutton-Chen potential for Cu (Ref. 15), and the tight-binding model for Ag.[16] All these models give a reasonably good description of phonon spectra for the corresponding bulk systems. Nanocrystals containing 459, 675, 887, and 959 atoms are studied. After the structural optimization,[17] the vibrational DOS is calculated through diagonalizing the dynamical matrices.

In order to pursue the spatial distribution of the elastic and vibrational properties, we divide the nanocrystal into geometry shells from the center of the mass to the surface, and each shell has the equal thickness of 1 Å. With the use of the calculated eigenmodes, we can calculate the average frequency $\langle f_I \rangle$ of the shell I by

$$\langle f_I \rangle = \sum_i^{3N-6} \omega_i \langle A_I^2 \rangle_i , \tag{1}$$

where N and ω_i are the total atoms in the nanocrystals and the ith eigenfrequency, respectively. $\langle A_I^2 \rangle_i$, the square amplitude of the ith eigenvector in shell I, is given by

$$\langle A_I^2 \rangle_i = \sum_n^{N_I} (A_i^n)^2 / N_I , n \subset N_I , \tag{2}$$

where N_I and A_i^n are the number of atoms in the shell I and the projected component of the ith renormalized eigenvector A_i on the nth atom, respectively.

A spatially localized mode decays exponentially outside the region. To quantify the spatial localization of modes, we calculate the projected vibrational DOS $\rho_I^*(\omega)$ of the shell I:

$$\rho_I^*(\omega) = \sum_i^{3N_I} \delta(\omega - \omega_i)\, \theta(\langle A_I^2 \rangle_i) / 3N_I , \tag{3}$$

where

$$\theta(\langle A_I^2 \rangle_i) = \begin{cases} 1, & \langle A_I^2 \rangle_i \geqslant C_0 (1 - \langle A_I^2 \rangle_i) \\ 0, & \langle A_I^2 \rangle_i < C_0 (1 - \langle A_I^2 \rangle_i). \end{cases} \tag{4}$$

C_0 is a constant larger than one. We choose 1.5 in our calculations.

In comparison, we also calculate the local vibrational DOS of the shell I, ρ_I, by:

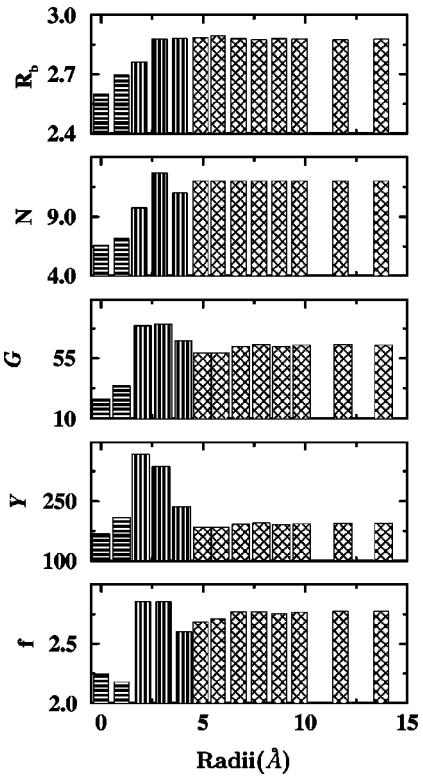

FIG. 1. The calculated local elastic constants (in units of GPa), Young's moduli (Y) and and shear moduli (G), the average local frequency (f, in units of THz), the average coordinates (N), and the average bond length (R_b, in units of Å) of each shell Au_{887}. The classification of the three regions is marked with horizontal, vertical, and net lines for the surface shell, transition shell, and core region, respectively. The lower-average local frequency in surface shell and higher-average local frequency in transition shell are not simply due to the changes of the bond length, but involving the many-body effect in contrary with previous suggestions.

$$\rho_I(\omega) = \sum_i^{3N-6} \langle A_I^2 \rangle_i \delta(\omega - \omega_i). \tag{5}$$

Different from the projected vibrational DOS, here the local vibrational DOS has the contribution of all the vibrational modes of a whole nanocrystal.

Shown in Fig. 1 are the average elastic constants, the average coordinates, average bond length, and average local vibrational frequency for each shell of Au_{887} nanocrystal. The local elastic constants are calculated by using the similar formula given by Egami, Maeda and Vitek.[18,19] As seen from Fig. 1, the nanocrystal can be classified into three regions according to the elastic and vibrational frequency discontinuities, as the surface shell, the transition shell, and the bulklike core region. It is readily observable that the surface shell is characterized by a much smaller local shear moduli, implying the softness of the shell. In contrast, the transition shell is characterized by high stiffness. This prototype example demonstrates that the nanocrystal has a well-defined physical surface separated by a hard transition shell from the core region. In all studied metallic nanocrystals in this report, we have found similar behavior.

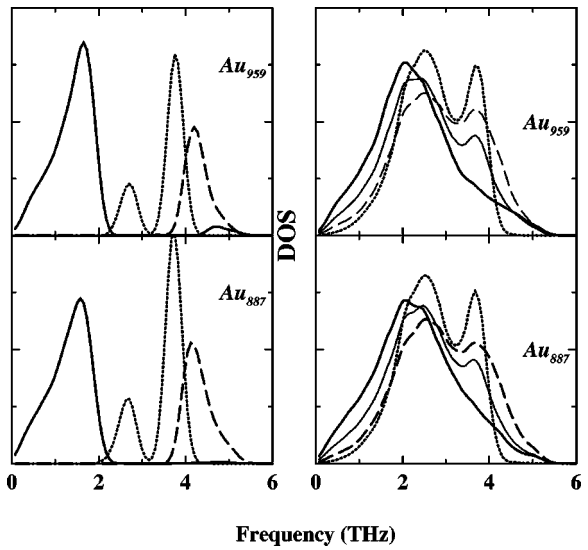

FIG. 2. Left: The projected vibrational DOS for surface (solid line), transition (dash line), and core (dot line) regions. Right: Local vibrational DOS for surface shell (thick solid line), transition shell (dash line), core region (dot line), and the total DOS (thin solid) for Au_{887} and Au_{959} nanocrystals.

The enhancement of the high-frequency modes is not simply due to the changes of the bond length as previously suggested.[1,2] From this figure, we can see that the main contribution to the high-frequency modes is from the transition region, however, the shortest average bond is not at the transition region; the surface shell has the shortest average bond length, and it has the lowest average local vibrational frequency. So, the shortening of the nearest bonding cannot fully account for the enhancement of the high-frequency modes. The physical reason for the enhancement of the low-frequency and high-frequency modes could be the softening and hardening of the elastic field. The hard elastic field in transition region may be from the over coordinations.

The enhanced high- and low-frequency modes are predominantly localized in the transition and surface shells, respectively. In Fig. 2 (left panel), we present the projected vibrational DOS for the above-mentioned three regions. The projected vibrational DOS of the surface shell dominant the low frequency and peaks at lower frequencies than the transitive peak of bulk gold. This indicates that most low-frequency modes are spatially localized in the thin surface shell. Owing to the fact that the physical surface is very thin (for Au nanocrystal it is about 2 Å), it behaves like a quasi-two-dimensional system. This has an important consequence for the interpretation of the experimentally observed linear frequency dependence of the vibrational DOS spectra. The origin of the low-frequency modes can be understood from the small elastic constants in the surface shell.

The projected vibrational DOS in the transition shell provide additional localized high-frequency modes outside of the highest-frequency of bulk gold. The origin of the enhanced high-frequency modes can be attributed to the elastic stiffening in the transition shell, consistent with the suggestions by Wolf and co-workers.[1] Since both surface and transition shells are thin, the fraction number of the atoms in

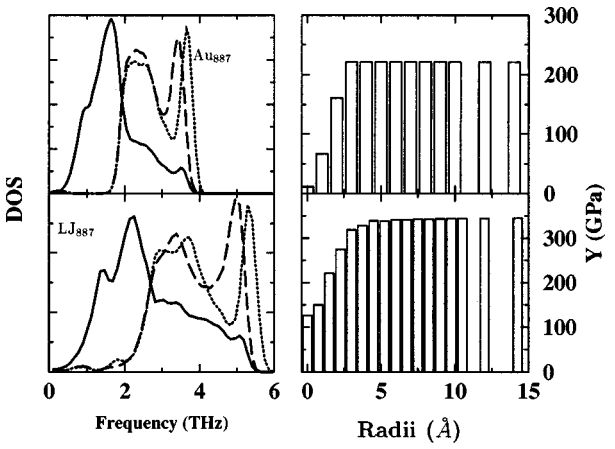

FIG. 3. Left: Local vibrational DOS for surface shell (thick solid line), transition shell (dash line), core region (dot line) for unrelaxed Au_{887} and relaxed LJ_{887} nanocrystals. Right: The calculated local Young's moduli (Y) (in units of GPa), as a function of the distance from surface to center. It can be seen there is not any transition shell in these two nanocrystals; correspondingly, no linear behavior can be observed for the surface shell.

these regions reduces inversely with the size of the nanocrystal. As a result, the enhanced low- and high-frequency modes scale with the inverse of the nanocrystal size. However, since the atoms in the surface shell reduce slower than that in the transition shell, the reduction of low-frequency modes with the increasing of the nanocrystal size will be slower than that of the high-frequency modes.

The prediction that the enhancement of low-frequency modes scales approximately inversely with the size of the nanocrystal is in excellent agreement with the recent inelastic neutron-scattering measurements of the Ni_3Fe nanocrystal DOS.[11] In contrast, the enhancement of high-frequency modes mainly arises from vibrational modes in the transition region, leading to a size dependence rather than linear, as observed experimentally. As expected, the core region has the similar DOS as the bulk one. We also show the calculated local vibrational DOS and total DOS for Au nanocrystals in Fig. 2 (right panel). Comparing the local DOS with the projected DOS in Fig. 2 (left panel), we find that the local DOS of the surface shell almost has the similar linear behavior as the projected DOS of the surface shell. Usually, the local DOS is not only due to the contribution of the localized modes, but also the contribution of all the other modes. This implies that one cannot simply explain the linear behavior of the local DOS for surface shell in term of the two-dimensional character of the surface, unless the local DOS mainly comes from the contribution of the localized modes. This is the case in the nanocrystal. This is why the obtained local surface DOS for nanocrystals in both experimental[3] and theoretical[2] work shows evident linear behavior. It is also observable that, at low-frequency region, the total DOS almost have similar linear behavior as the local DOS of the surface shell. These results prove additional evidence for the previous statement that the low-frequency modes predominantly come from the surface shell, while the enhancement of high-frequency modes are mainly due to the vibration modes in the transition shell.

The presence of the transition shell is the key of the presence of the linearity and high-frequency tails. We have calculated some unrelaxed Au and LJ clusters (see Fig. 3), where there is not any transition shell, none of them shows the linear behavior and the additional high-frequency tails in the density of states. Thus, it is the transition shell that makes the surface shell show a two-dimensional behavior.

The linear dependence of the projected vibrational DOS on frequency for the surface shell remains intact for different metals and different sizes. Figure 4 shows the projected vibrational DOS of the surface shell for different metals (Ag, Au, Cu, and Pb with 459 atoms), as well as for different size of Au nanocrystals ($N=459$, 675, 887, 959). In view that the studied metal has different elastic properties, the associated projected vibrational DOS has different slope at low frequency. In contrast, the projected vibrational DOS is independent of the size of the nanocrystal as they have the same slope. The similar behavior has also been observed for other metallic nanocrystals.[19]

The linear behavior of the projected DOS of the surface should be presented not only in the surfaces of nanocrystals but also in the surfaces of bulk materials. However, the previous experimental and theoretical work mainly concentrated in the local DOS of the surface, which includes much more of the contribution of the nonsurface modes. Additionally,

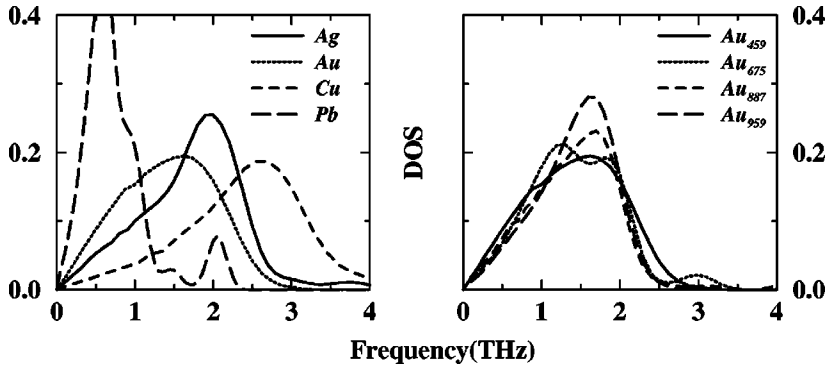

FIG. 4. Left: the projected vibrational DOS of surface shell for various metallic nanocrystals with 459 atoms. Right: the projected vibrational DOS of surface shell for Au nanocrystals of different sizes.

the linear behavior of bulk surface is generally much weaker than that in nanocrystals. This comes from two aspects. First, bulk surfaces have much higher shear moduli than that in nanocrystals, which makes the slope of the linear much smaller in bulk surface. Second, the transition shell in bulk material is not as hard as that in nanocrystals.

In summary, we have studied the unusual vibrational properties of metallic nanocrystals. Our results show that there exist three regions for metallic nanocrystals: a soft surface shell, a hard transition shell, and a bulklike core region. The enhanced low- and high-frequency modes are spatially localized in two shells. The enhanced low-frequency modes are mainly attributed to the atoms in the soft surface shell, while the enhanced high-frequency modes are predominantly attributed to the atoms in the stiff transition shell. The linear behavior of surface atoms results from the quasi-two-dimension character.

This work was supported partially by Air Force Office of Scientific Research under Grant No. F49620-96-1-0211 and Army Research Office under Grant No. DAAH04-95-1-0651, also supported partially by NNSF of China, CAS project and special fund for major state basic research project.

[1] D. Wolf, J. Wang, S.R. Phillpot, and H. Gleiter, Phys. Rev. Lett. **74**, 4686 (1995); J. Wang, D. Wolf, S.R. Phillpot, and H. Gleiter, Philos. Mag. A **73**, 517 (1996).
[2] A. Kara and T.S. Rahman, Phys. Rev. Lett. **81**, 1453 (1998).
[3] U. Stuhr, H. Wipf, K.H. Andersen, and H. Hahn, Phys. Rev. Lett. **81**, 1449 (1998).
[4] K. Suzuki and K. Sumiyama, Mater. Trans., JIM **36**, 188 (1995).
[5] B. Fultz, L. Anthony, L.J. Nagel, R.M. Nicklow, and S. Spooner, Phys. Rev. B **52**, 3315 (1995).
[6] B. Fultz, J.L. Robertson, T.A. Stephens, L.J. Nagel, and S. Spooner, J. Appl. Phys. **79**, 8318 (1996).
[7] B. Fultz, C.C. Ahn, E.E. Alp, W. Struhrhahn, and T.S. Toellner, Phys. Rev. Lett. **79**, 937 (1997).
[8] H.J. Fecht, Phys. Rev. Lett. **65**, 610 (1990).
[9] M. Wagner, Acta Metall. Mater. **40**, 957 (1992).
[10] H. Frase, L.J. Nagel, L.J. Robertson, and B. Fultz, Philos. Mag. B **75**, 335 (1997).
[11] H. Frase, B. Fultz, and J.L. Robertson, Phys. Rev. B **57**, 898 (1998).
[12] J. Trampenau, K. Bauszuz, W. Petry, and U. Herr, Nanostruct. Mater. **6**, 551 (1995).
[13] F. Ercolessi, M. Parrinello, and E. Tosatti, Philos. Mag. A **58**, 213 (1988).
[14] D.Y. Sun, Y. Xiang, and X.G. Gong, Philos. Mag. A **79**, 1963 (1999).
[15] A.P. Sutton and J. Chen, Philos. Mag. Lett. **61**, 139 (1990).
[16] Fabrizio Cleri and Vittorio Rosato, Phys. Rev. B **48**, 22 (1993).
[17] F. Ercolessi, W. Andreoni, and E. Tosatti, Phys. Rev. Lett. **66**, 911 (1991).
[18] T. Egami, K. Maeda, and V. Vitek, Philos. Mag. A **41**, 993 (1980).
[19] D. Y. Sun and X. G. Gong (unpublished).